

BULETINUL INSTITUTULUI POLITEHNIC DIN IAȘI  
Publicat de  
Universitatea Tehnică „Gheorghe Asachi” din Iași  
Tomul LIX (LXIII), Fasc. 2, 2013  
Secția  
ELECTROTEHNICĂ. ENERGETICĂ. ELECTRONICĂ

## NEW POSSIBILITY IN MONITORING AND DIAGNOSES OF ELECTRICAL EQUIPEMENT

BY

**MONICA ATUDORI\***

“Gheorghe Asachi” Technical University of Iași  
Faculty of Electrical Engineering

Received: May 7, 2013

Accepted for publication: June 24, 2013

**Abstract.** The paper presents a new possibility of using the electromagnetic map of electrical equipment in monitoring, diagnoses, controlling and commanding them. The mathematical modeling and simulation of different operating status of the electrical equipment was accomplished in EMTP-ATP software. Are also presented results of the monitoring and diagnoses of the electrical equipment using the 6024 E National Instruments acquisition board.

**Key words:** electromagnetic map; electrical equipment and devices; electromagnetic field; acquisition board.

### 1. Introduction

The technological progress of data transmission and the development and expansion of power systems worldwide were a major factor in increasing the electromagnetic field level as well as the bio-organism and human body exposure to the electromagnetic radiation.

The purpose of this paper is to apply new possibilities of monitoring and diagnosing of electrical equipment using their own electromagnetic radiation field.

With the help of advanced software/hardware structure we've been able

---

\* *e-mail:* monica.atudori@ee.tuiasi.ro

to study the behavior of electrical equipment and their influence on the environment throughout the electromagnetic map.

## 2. Methods

The electromagnetic field is generated by each electrical equipment and installation, which can lead to different kinds of perturbations in the equipment functioning or other equipment nearby (overvoltage, overcurrents, excessive heating of high voltage power line conductors). In the chapter below are described some of the equipment that make part of our study, highlighting the parameters that have been analyzed.

### 2.1. Electric Motors. Star–Delta Starting

All indirect starting methods are used to reduce the starting current. In the case of a star – delta starting the network voltage is applied directly to the star connected to a three phase winding coil. (*Basics for practical operation*, 1998).

Effective line current for a steady state on a star connection is described by the expression:

$$I_{IY} = I_{fY} = \frac{U_{fY}}{Z_f} = \frac{U_l}{\sqrt{3}Z_f}. \quad (1)$$

The effective current expression for a delta connection changes to

$$I_{I\Delta} = \sqrt{3}I_{f\Delta} = \frac{\sqrt{3}U_{f\Delta}}{Z_f} = \frac{\sqrt{3}U_l}{Z_f}. \quad (2)$$

The absorbed current report for the two connections has the value

$$\frac{I_{IY}}{I_{I\Delta}} = \frac{3}{3}. \quad (3)$$

Due to a  $\sqrt{3}$  time mitigation of the phase voltage while in star connection, the starting torque is also three times lower than the direct starting case; the electromagnetic torque is proportional with the square stator phase voltage. This inconvenient is limiting the application of the star-delta starting only in the situation of an unloaded start of a motor or a low resistant static torque.

The star–delta starting method is used for non-synchronic short-circuit three phase motors, with a nominal power between 5.5...14 kW/400 V (Hortopan, 1967). This method can be used only in the case of the motors that have the nominal phase voltage equal to the three phase network line voltage. The mechanical characteristic of the star–delta starting is shown in the Fig. 1.

The star–delta starting method is very efficient from the technical and economical point of view, that's why it has a large application scale in power engineering.

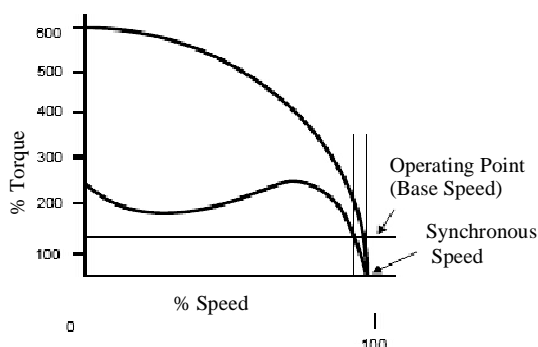


Fig. 1 – Electric characteristic of star–delta motor starting.

## 2.2. Fuses

The fuses are designed to protect the circuit against overload and short circuit. Depending on the current they are able to break (<1 kA to >1 kA); there are different types of fuses. The technical characteristic of a fuse are listed below:

- nominal current ( $I_n$ );
- nominal voltage ( $U_n$ );
- breaking capacity – the maximum short-circuit current that can be break according to standard normative;
- time – current characteristic  $t = f(I)$  is shown in Fig.2.;  $t$  represent the melting time of the fuse element + the arcing time = the breaking time.

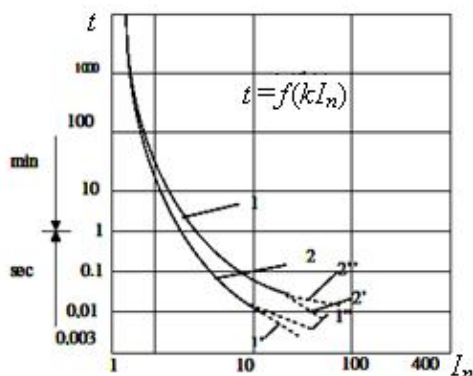


Fig. 2 – Time – current characteristic.

The shape of the characteristic differs depending on fuse type. The main difference is due to the breaking time: there are slow fuses, fast fuses, mix fuses and ultra – fast fuses.

For a current 15 times bigger than  $I_n$  the breaking time of the fuse is very short, the circuit being disconnected before the short-circuit current reaches its maximum value.

### 3. Modeling and Simulation of Electrical Equipment

Modeling and numeric simulation allows us to study and evaluate the electro-mechanic systems behavior in the applications they were designed for, but also for other application, which leads to the development of new types of systems and equipments.

The electromagnet (Fig. 3) is one of the most important electro-mechanic systems. This device plays a significant role in the interconnections of two subsystems, where the first system, with electric output signal, controls the second one with a mechanical input signal.

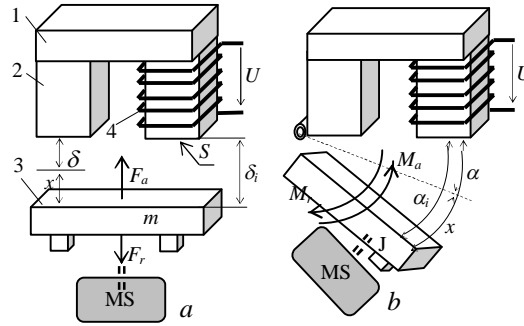


Fig. 3 – Air-gap zone: *a* – transition mobile armature;  $\delta$  – linear air-gap;  $x$  – motion;  $m$  – reduce weight;  $F_r$  – resistant force; MS – mechanic subsystem; *b* – tilting mobile armature;  $\alpha$  – angular air-gap;  $J$  – inertia moment.

In Fig. 3 *a* the direct current electromagnet has a transition mobile armature; in Fig. 3 *b* it has a mobile tilting armature. Depending on the armature type, its motion during the transient state is described by one of the following eqs. (Baraboi *et al.* 1996):

$$\begin{cases} m \frac{d^2x}{dt^2} + a_t \frac{dx}{dt} + e_t x = F_a(x) - F_r(x), \\ J \frac{d^2\alpha}{dt^2} + a_b \frac{d\alpha}{dt} + e_b \alpha = M_a(x) - M_r(x), \quad x(0) = x_0, \quad \left. \frac{dx}{dt} \right|_0 = 0, \end{cases} \quad (4)$$

where  $a_t$ ,  $a_b$  and  $e_t$ ,  $e_b$  are the damping and, respectively, elastic constants of the electro-magnet. The active force,  $F_a$ , and the active moment,  $M_a$ , are given by relations

$$F_a = 2F_\delta = \frac{\Phi_\delta^2}{\mu_0 S_\delta}, \quad M_a = rF_\delta, \quad (5)$$

where:  $F_\delta$  is the active force reported to the air gap,  $r$  – force arm,  $\Phi_\delta$  – magnetic flow of the air gap,  $S_\delta$  – polar surface. The eq. (5) is used to calculate the active force and moment for the electromagnet described in Fig. 3 a.

The electric circuit single line diagram of the direct current electromagnet is shown in Figs. 4 a and 4 b.

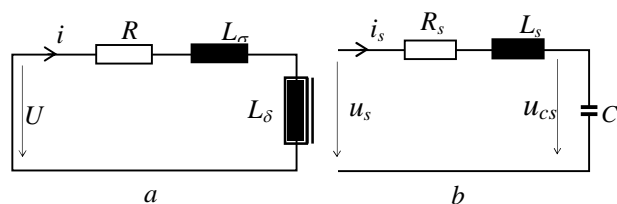


Fig. 4 – Single line diagram: *a* – electromagnet:  $R$  – resistance,  $L_\sigma$  – dispersion inductance,  $L_\delta$  – inductance of the magnetic flow,  $U$  – voltage,  $i$  – current; *b* – simulation mode.

The electrical parameters in Fig. 4 *b* are the same as in Fig. 4 *a*, but calculated according to the mathematic model. This circuit is described by eqs.

$$\begin{cases} U = Ri + L_\sigma \frac{di}{dt} + N \frac{d\Phi_\delta}{dt}, \\ \theta = Ni + \theta_F, \quad \theta_F = -K \frac{d\Phi_\delta}{dt}, \end{cases} \quad (6)$$

where:  $\theta_F$  is the solenation that corresponds to Foucault currents,  $N$  – number of coil coilings and  $K$  – constant coefficient.

### 3.1. Numerical Simulation in EMPT – ATP

The mathematic model of the direct current electromagnet functioning is based on a differential eqs. system, from which one correspond to the mobile armature motion and the others to the electric circuit functioning. For an electromagnet with mobile armature, the model is based on the eqs. (4),..., (6). The electromagnetic field is characterized, in a certain point in space, by the superposition of an electric and magnetic field, variable in time, which are mutual generating. The state of the electric field is described by two vectors:  $\mathbf{E}$  – the intensity of the electric field and  $\mathbf{D}$  – the electric induction. The magnetic field state is described by  $\mathbf{B}$  – magnetic induction and  $\mathbf{H}$  – magnetic field intensity (David *et al.*, 2006).

The numerical simulation is performed with the EMTP - ATP software and the graphical results are shown with the help of the MC's Plot XY, in Figs. 5 and 6.

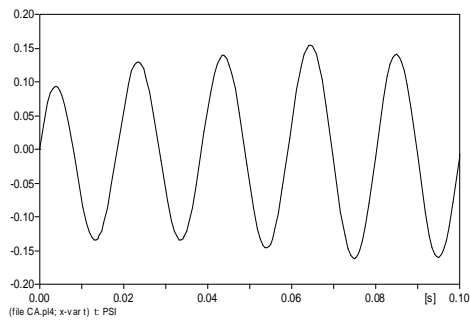


Fig. 5 – Transient regime of the magnetic flux.

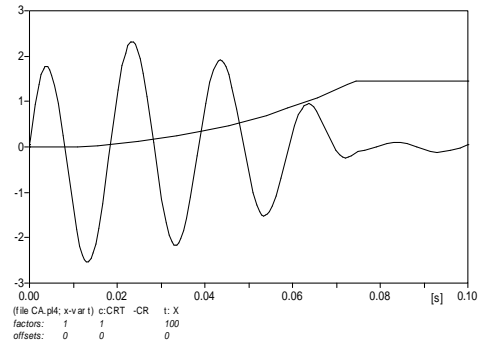


Fig. 6 – Current absorption of the coil and armature motion.

### 3.2. Electrical Fuse Modeling

The simulation of an electrical fuse behavior throughout its own electromagnetic radiation field was possible with the help of EMTP - ATP software. For modeling a fuse the next steps must be followed:

- a) drawing up the equivalent electric scheme – RC type that is simulating the heat release and thermal transfer phenomena in its volume;
- b) establishing of the input data;
- c) generate heating and arc extinction curves as output data.

The ATP Draw model of an electric fuse is shown in Fig. 7 as well as the parameters of interest like melting time and melting temperature (shown in Plot XY application).

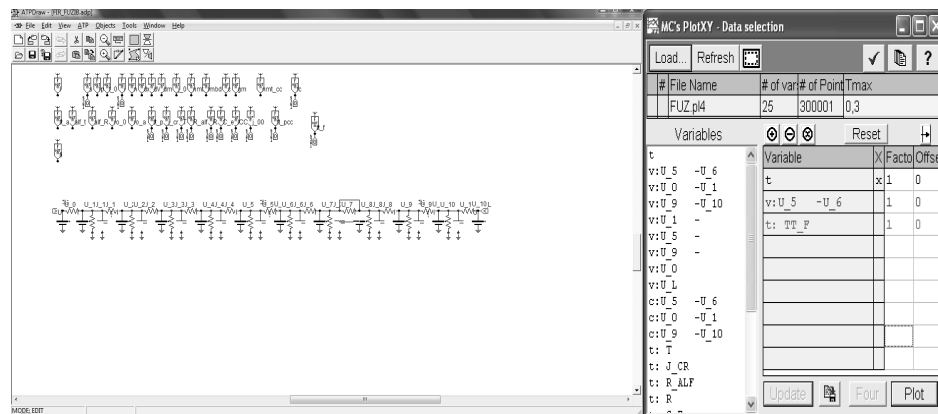


Fig. 7 – ATP Draw model and Plot XY variables for an electrical fuse.

Graphical results for a 40 A electrical fuse model are presented in Fig. 8. The mathematical model was created in order to calculate the melting time of the fuse strip when a fault occurs.

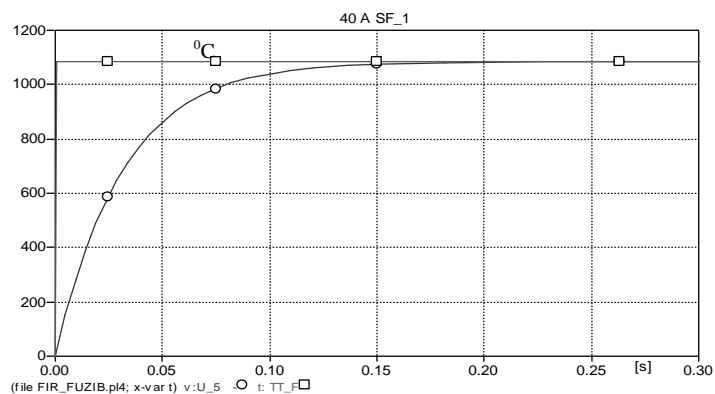


Fig. 8 – Modeling results: melting time, melting temperature.

#### 4. Experimental Procedure

In order to distinguish the influence of the electromagnetic field on the electrical equipment the monitoring and diagnoses techniques were applied for fuses and electric motors.

The acquisition system used to capture and therefore analyse the information stored (contained) in the electrical fuse own electromagnetic radiation field is composed of: the NI 6024 E acquisition board, one up to three magnetic sensors, a LabView application.

The block diagram of the acquisition system is presented in Fig. 9.

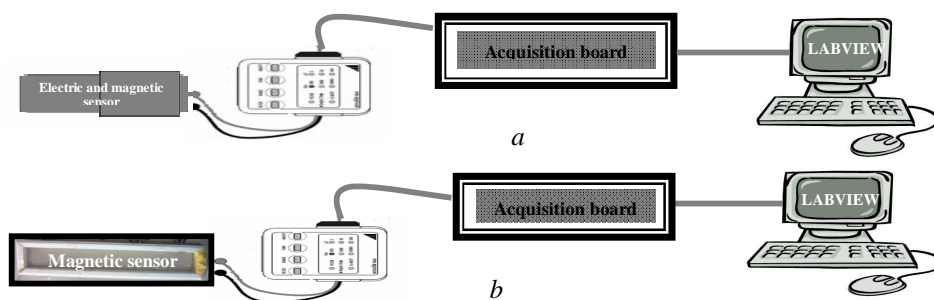


Fig. 9 – Block diagram of acquisition system: *a* – magnetic sensor MetraHit 28 s;  
*b* – coil probe.

#### 5. Experimental Results

The experiments presented in this paper were conducted for a star – delta motor and for different types of fuses.

### 5.1 Results at the Star-Delta Motor Starting

The graphical results are presented in the Figs. 10,...,12.

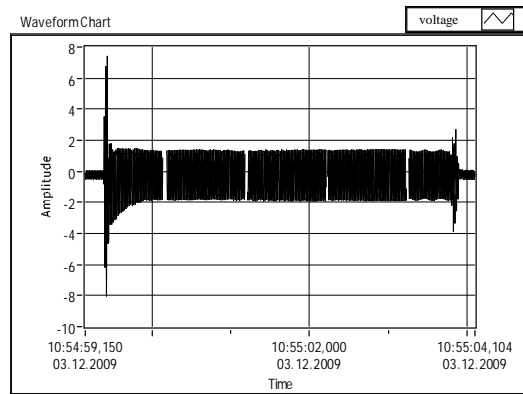


Fig. 10 – Star-delta motor starting.

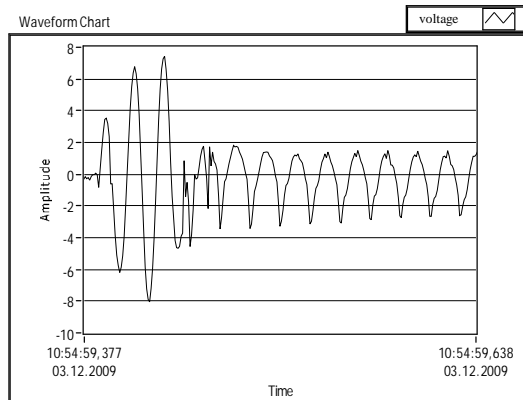


Fig. 11 – Contactor starting.

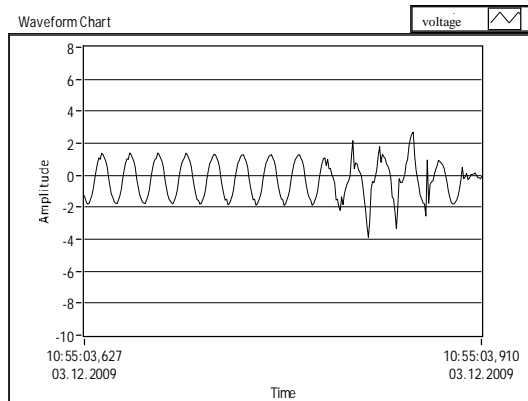


Fig. 12 – Contactor stop.

The time of the star – delta starting, opening and closing of the contactor and the signal amplitude for each of these operations are shown in Table 1.

**Table 1**  
*Signal Amplitude – Service Time*

	Time, [s]	Amplitude, [V]
Star–delta starting	4.989	15
Contactor starting	0.261	15.8
Contactor stop	0.283	7

## 5.2. Results on Testing Electrical Fuses Using one Magnetic Sensor

The data was captured with the help of an acquisition board and processed in a LabView application (Rotariu, 2009). The electrical fuse installation submitted to laboratory testing is shown in the Fig.13.

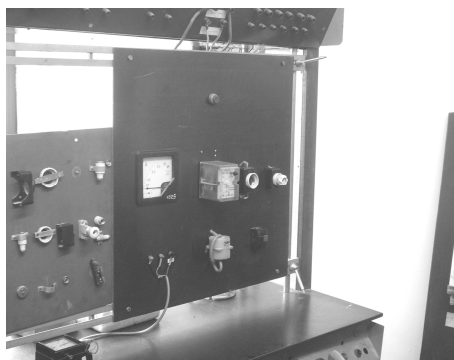


Fig. 13 – Electrical fuse panel.

The measurements of magnetic induction were applied for a fuse operation at different current values (40, 60 and 80 A). Graphical results are shown in Figs. 14,...,16.

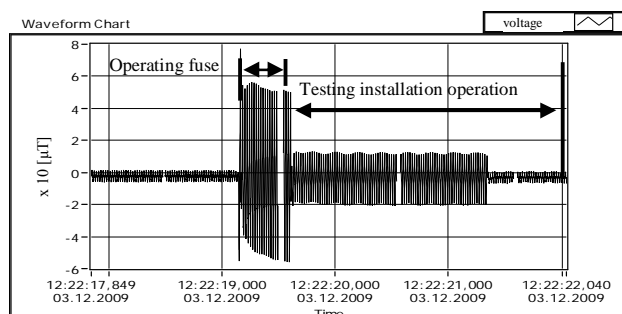


Fig. 14 a – Capture of magnetic induction – 40 A.

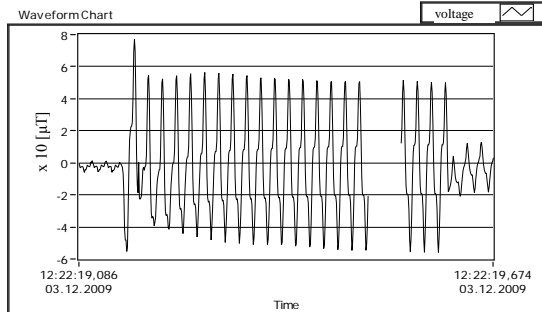


Fig. 14 b –Fuse operating status – 40 A.

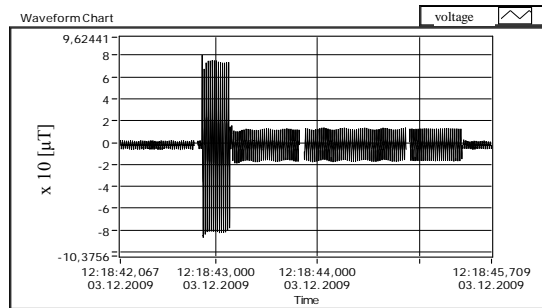


Fig. 15 a – Capture of magnetic induction – 60 A.

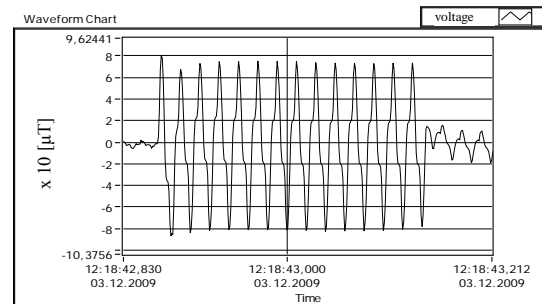


Fig. 15 b – Fuse operating status – 60 A.

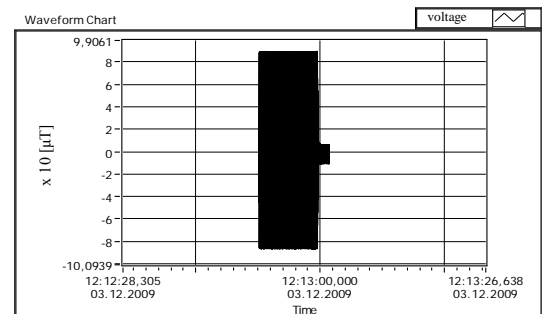


Fig. 16 a – Capture of magnetic induction – 80 A.

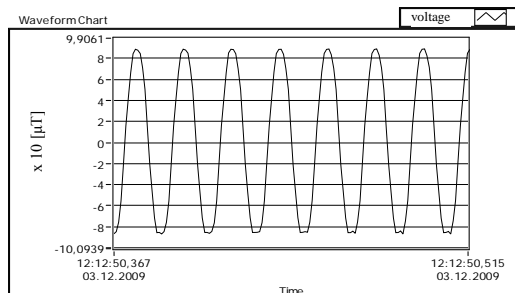


Fig. 16 b – Fuse operating status – 80 A.

For a 40 A current the fuse operating time was 0.461 s. At higher current intensity the operating time diminished to about 0.15 s. The exact operation time and the breaking current values are shown in Table 2.

**Table 2**  
*Electric Fuse Operating Time for Different Current Values*

Current, [A]	Time, [s]
40	0.461
60	0.279
80	0.148

### 5.3. Results on Testing Electrical Fuses Using Magnetics Sensors

In this case two types of electrical fuses were used: one with 2 strips and the other with 4 strips. Both fuses were tested for a 100 A current. Two channels (C0 and C1) on the acquisition board were allocated for the monitoring

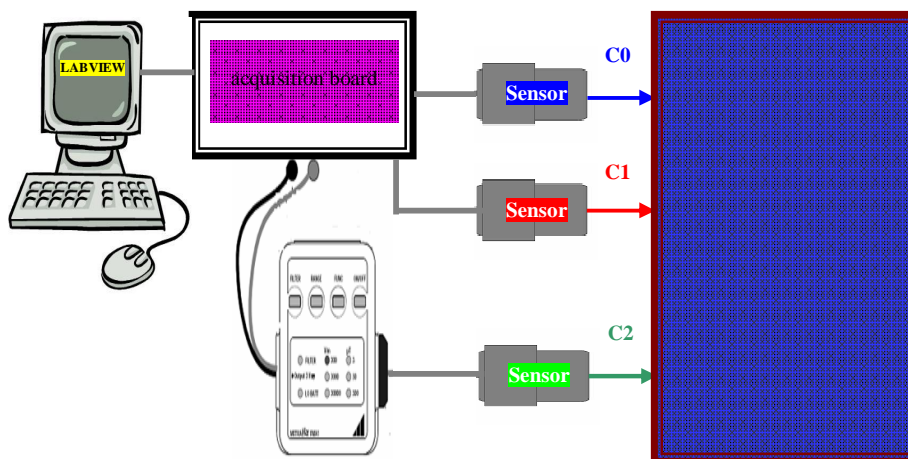


Fig. 17 – Block diagram of a three channel acquisition system.

of the magnetic field and another channel (C2) for the monitoring of the electric field. Measuring the electric field was possible after the sensor calibration and with the help of MetraHit 28 s device. The block diagram of the acquisition system is shown in Fig. 17.

In Figs. 18, 19 *a* and 19 *b* are showing the data captured for a two strips fuse at 100 A.

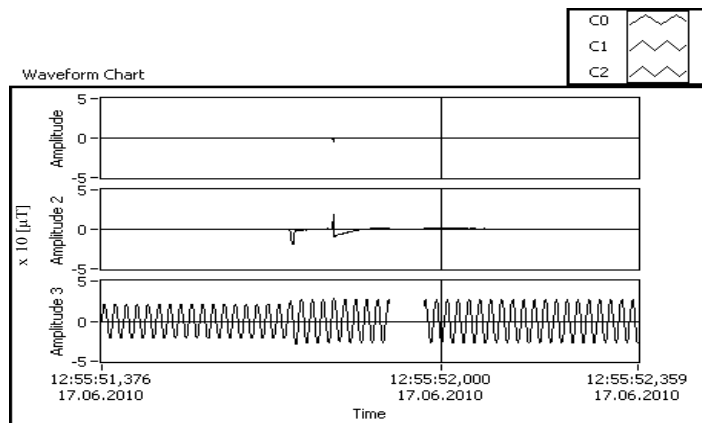


Fig. 18 – Fuse operating status – 100 A – 2 strips.

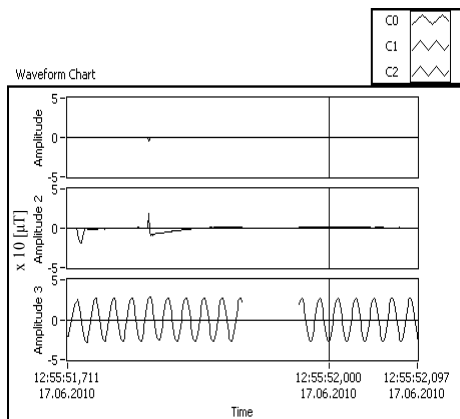


Fig. 19 *a* – Installation started.

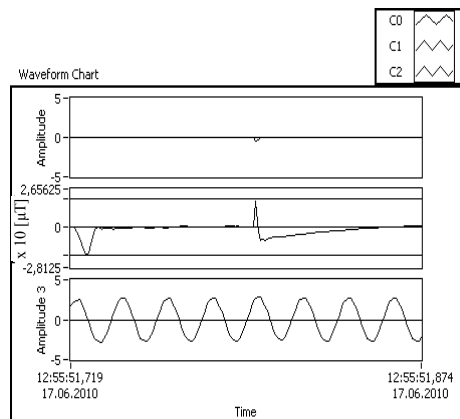


Fig. 19 *b* – Installation stoped.

In Figs. 20, 21 *a* and *b* are showing the data captured for a four strips fuse at 100 A.

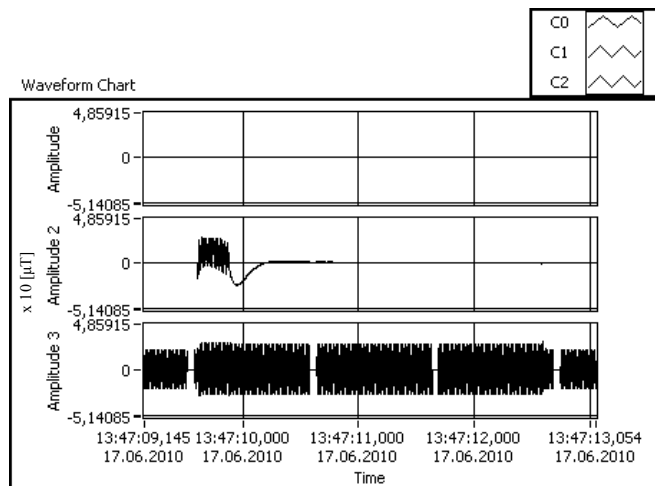


Fig. 20 – Fuse operating status – 100 A – 4 strips.

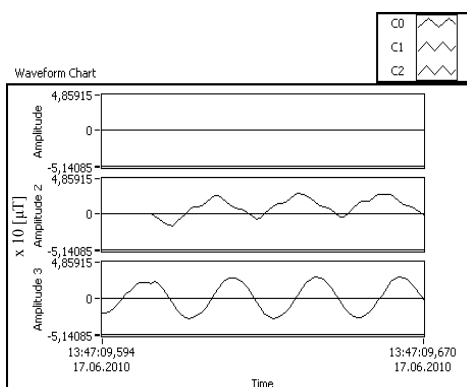


Fig. 21 a – Installation started.

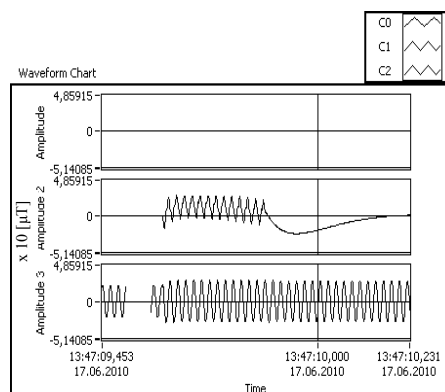


Fig. 21 b – Installation stopped.

The results on the two types of fuses are shown in Table 3.

**Table 3**  
*Operating Time for 2 and 4 Strips Fuses*

	Time, [s]
2 strips fuse	0.029
4 strips fuse	0.259

For the two types of fuses tested in the lab, the use of electric field from channel C2, allows visualization of start and stop moments of the installation operation process.

Another important aspect is the zero value of the magnetic field captured on channel 0 which means, from the biocompatibility perspective, that the working environment is not dangerous for the operating staff.

## 6. Conclusions

The paper presents new possibilities in the monitoring and diagnoses of the electrical equipment using their own electromagnetic radiation field. The present study was based especially on a successive functioning of the equipment (motor star – delta starting) obtaining this way a very good accuracy of the registered data.

The values of the electromagnetic field give us information on the human body and environment exposure to these fields. That is why analyzing the information contained in the electromagnetic map of the electrical equipment is an important step in the monitoring and diagnoses techniques.

## REFERENCES

- Baraboi A., Adam M., Ciutea I., Hnatiuc E., *Tehnici moderne în comutația de putere*. Edit. A 92, Iași, 1996.
- David V., Crețu M., *Măsurarea intensității câmpului electromagnetic – Teorie și aplicații*. Casa de Editură Venus, Iași, 2006.
- Hortopan G., *Aparate Electrice*. Edit. Did. și Pedag., București, 1967.
- Rotariu M., *Experimental and Theoretic Basis of Electromagnetic Radiation Field Used in Monitoring and Diagnose Electrical Equipment and Installation*. Ph. D. Diss. Report, Techn. Univ. “Gh. Asachi”, Iași, 2009.
- \* \* *Basics for Practical Operation, Motor Starting, Traditional Motor Starting, Soft Starters, Frequency Inverters*. Publ. WP Start, EN, 1998.

## POSSIBILITĂȚI NOI DE MONITORIZARE ȘI DIAGNOSTICARE A ECHIPAMENTELOR ELECTRICE

(Rezumat)

Se prezintă posibilitatea utilizării câmpului electromagnetic al echipamentelor electrice în scopul monitorizării, diagnosticării, controlului și comandării acestora. Modelul matematic și simularea diferitelor stări de funcționare au fost realizate cu ajutorul softului EMTP – ATP. Obținerea rezultatelor, monitorizarea și diagnosticarea echipamentelor electrice a fost posibilă prin utilizarea unui sistem de măsură format din trei componente: LabView, placa de achiziție 6024 E National Instruments, senzori magnetici.